

# Distribution of Developmental Myosin Heavy Chains in Adult Rabbit Extraocular Muscle: Identification of a Novel Embryonic Isoform Absent in Fetal Limb

Christine Angela Lucas and Joseph Foon Yoong Hoh

**PURPOSE.** To identify embryonic and neonatal/fetal myosin heavy chains (MyHCs) in rabbit extraocular muscle (EOM) by electrophoretic and immunochemical analyses and to describe the distribution of these two MyHC isoforms in the endplate zone (EPZ) and the distal and proximal segments of EOM fibers.

**METHODS.** SDS-PAGE and Western blot analysis using monoclonal antibodies (mAbs) against embryonic and neonatal/fetal MyHCs were performed on MyHC isoforms from rabbit adult and neonatal EOM and fetal limb muscles. Immunohistochemical analysis was performed along the entire length of the rabbit superior rectus muscles, using these and other mAbs.

**RESULTS.** Western blot analysis showed that adult rabbit EOM had two embryonic MyHC bands: a weakly stained band that comigrated with the embryonic MyHC from fetal limb muscles, and a strongly stained band of lower electrophoretic mobility for which there was no limb counterpart. Three anti-embryonic MyHC mAbs stained muscle fibers, predominantly in the orbital layer, and staining was localized distal and proximal to the EPZ but not in the EPZ itself. There, most fibers expressed the EOM-specific fast MyHC, although some fibers expressed  $\alpha$ -cardiac MyHC. Anti-neonatal/fetal MyHC mAb failed to stain in Western blot analysis but stained scattered fibers predominantly in the global layer, and there was no specific absence of staining at the EPZ.

**CONCLUSIONS.** There are two electrophoretically distinct isoforms of embryonic MyHCs in adult rabbit EOM. These isoforms are expressed in orbital fibers but are excluded from the EPZ, where EOM-specific fast MyHC is strongly expressed. Neonatal and fetal MyHC is weakly expressed in the EOM, but is not excluded from the EPZ. (*Invest Ophthalmol Vis Sci*. 2003;44:2450–2456) DOI:10.1167/iovs.02-1109

EOMs are a group of highly specialized muscles with very complex functions. EOM fibers differ from limb muscle fibers, in morphology, physiology, and biochemistry.<sup>1</sup> The concept that EOMs are a separate muscle allotype,<sup>2</sup> distinct from limb and jaw muscle allotypes,<sup>3</sup> received strong support from the recent DNA microarray analysis, which revealed that EOM and limb muscles differ strongly in the pattern of gene expression.<sup>4</sup> A functionally important aspect of this difference is the expression of myosin genes. Adult EOM fibers express MyHC

isoforms found in adult limb fast (2A, 2X, and 2B MyHCs) and slow (type 1/ $\beta$  MyHC) fibers,<sup>5,6</sup> but they express additional developmental isoforms (embryonic and neonatal/fetal MyHCs) found only in immature limb muscles,<sup>6</sup> the cardiac  $\alpha$ -MyHC,<sup>7,8</sup> and two extraocular (EO)-specific isoforms, the EO-fast MyHC<sup>2,9</sup> and the slow-tonic MyHC.<sup>10,11</sup>

EOMs are organized into two layers: a thin orbital layer and a more substantial global layer. Fibers in the orbital layer are of two types—singly innervated fibers (oSIFs) and multiply innervated fibers (oMIFs)—both of which vary in structure along their length. Close to the middle of oMIFs, there is a large endplate in the region called the endplate zone (EPZ), with small, regular myofibrils characteristic of twitch fibers,<sup>12–15</sup> whereas the flanking end segments are multiply innervated and have large, ill-defined myofibrils typical of amphibian tonic fibers.<sup>12–15</sup> Most oMIFs show a decrease in diameter and myofibril size toward their middle and around the EPZ.<sup>12,13,16</sup> The oSIFs swell in diameter,<sup>12,14,15,17</sup> and show a decrease in myofibril size<sup>18</sup> in the EPZ. Correlated with structural variations, expression of MyHCs also varies systematically along the length of orbital muscle fibers. The interpretation of early studies of this phenomenon was plagued by the multiplicity of isoforms in the EOM and the lack of monospecific antibodies. Jacoby et al.<sup>19</sup> showed that an mAb against all fast MyHC isoforms stains both oSIFs and oMIFs in the EPZ of rat EOM. Distal and proximal to the EPZ, oSIFs continued to stain with this anti-fast MyHC mAb, but these regions also costained with an mAb against embryonic and neonatal MyHC isoforms, whereas oMIFs stained with the latter mAb only. The limitation of this study was that the mAbs used were relatively nonspecific—that is, one antibody could not distinguish between embryonic and neonatal MyHC isoforms and the other could not distinguish between the different isoforms of fast MyHCs. Rubinstein and Hoh<sup>20</sup> using monospecific mAbs, showed that embryonic MyHC is expressed in most orbital fibers distal and proximal to the EPZ, but not in the EPZ itself. In the EPZ, oSIFs express EO-specific fast MyHC and oMIFs express slow (type 1/ $\beta$ ) MyHC along their entire length. Neonatal MyHC may be expressed in only a few fibers in the EOM orbital layer in the rat.<sup>21</sup> A detailed analysis of MyHC expression along the length of orbital muscle fibers is not available.

In the rabbit EOM, oSIFs stain with a nonspecific mAb against fast MyHCs in the EPZ, and distally and proximally stain with both the anti-fast MyHC mAb and a nonspecific mAb against developmental MyHC isoforms.<sup>22,23</sup> oMIFs stain with a cardiac-specific  $\alpha$ -MyHC mAb in the EPZ and distally and proximally stain with both the cardiac-specific  $\alpha$ -MyHC and a nonspecific mAb against developmental MyHC isoforms.<sup>23</sup> In another study, the distal half of the rabbit EOM was studied immunohistochemically, using monospecific mAbs against embryonic and neonatal MyHCs.<sup>24</sup> The investigators showed that fibers expressing embryonic MyHC are more abundant in the orbital layer, whereas fibers expressing neonatal MyHC are more abundant in the global layer. They also found an increase in the number of fibers expressing embryonic MyHC toward the distal end of the EOMs.<sup>24</sup> A limitation of this study is that

From the Department of Physiology and Institute for Biomedical Research, University of Sydney, Sydney, New South Wales, Australia.

Supported by a grant from the National Health and Medical Research Council of Australia.

Submitted for publication October 30, 2002; accepted November 26, 2002.

Disclosure: C.A. Lucas, None; J.F.Y. Hoh, None

The publication costs of this article were defrayed in part by page charge payment. This article must therefore be marked "advertisement" in accordance with 18 U.S.C. §1734 solely to indicate this fact.

Corresponding author: Joseph Foon Yoong Hoh, Department of Physiology and Institute for Biomedical Research, F13, University of Sydney, Sydney NSW 2006, Australia; joeh@physiol.usyd.edu.au.

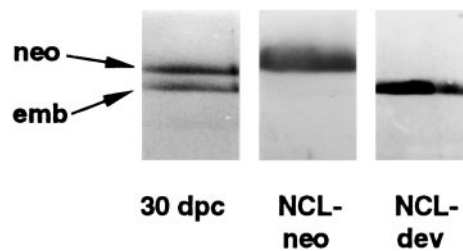


**FIGURE 1.** High-resolution SDS gels of MyHCs from rabbit 30-dpc limb muscles stained with Coomassie brilliant blue and corresponding Western blots stained with mAbs NCL-neo and NCL-dev.

the expressions of embryonic and neonatal MyHCs were determined without reference to the EPZ.

To date, electrophoretic and immunoblot analyses on MyHCs in EOMs have not clearly identified embryonic and neonatal MyHCs. SDS gel electrophoresis of rat EOM revealed five MyHC components.<sup>25</sup> A band migrating between 2X and 2B MyHC components was thought to be the neonatal MyHC, but this was not confirmed by immunoblot analysis. In addition, there was no mention of an embryonic MyHC component. In another study, Western blot analysis of developing and adult rat EOM MyHCs stained with an mAb against embryonic MyHC showed two positive bands, which suggests the presence of two isoforms.<sup>26</sup> It remains to be seen how the electrophoretic mobility of these two embryonic MyHC components are related to the other EOM MyHC components and how these apparent isoforms of embryonic MyHC are related to the limb embryonic and neonatal MyHCs.

Mechanical analysis of single rabbit EOM fibers revealed that values of the dynamic stiffness parameter  $f_{min}$ , that reflects the myosin cross-bridge cycling rate, form a continuum spanning values above and below those seen in fast limb fibers.<sup>27</sup> Because mechanical properties of muscle fibers are controlled to a large extent by MyHC isoform composition,<sup>28</sup> such a wide dynamic range of functional properties reflects the complex distribution of the nine different MyHCs. A systematic description of MyHC isoform composition along the length of the various EOM fiber types is called for before their functions can be unraveled. Toward this end, our laboratory has raised highly specific mAbs against MyHCs expressed in EOMs.<sup>2,29</sup> This work is the first of a series of immunochemical studies, and focuses first on identifying embryonic and neonatal/fetal MyHCs in rabbit EOM by SDS-PAGE and Western blot analysis and second on the distribution of these MyHC isoforms in the EPZ and flanking regions of orbital fibers in rabbit EOM.

## METHODS

### Tissue Preparation

Four adult New Zealand White rabbits (approximately 2 kg) were anesthetized and the extraocular, vastus lateralis, and tongue muscles were removed. The superior rectus (SR) muscles were dissected intact, with the distal ends attached to the sclera of the eye and the proximal ends attached to the sphenoid bone. The limb and EOMs were removed from two anesthetized rabbits of each of the following ages: 30 days post coitus (dpc), newborn, and 10 and 15 days old. The animals were maintained and used in accordance with the Australian Code of Practice for the Care and Use of Animals for Scientific Purposes and with the ARVO Statement for the Use of Animals in Ophthalmic and Vision Research. The adult rabbit SR muscles were mounted on cork with Tissue-Tek (Miles Scientific, Elkhart, IN), frozen in isopentane cooled in liquid nitrogen, and cut at  $-20^{\circ}\text{C}$  into  $10\text{-}\mu\text{m}$ -thick serial sections along the entire length of the muscle. The remainder of the

muscles were frozen and stored in liquid nitrogen for myosin extraction.

### Antibodies and Immunohistochemical Techniques

Indirect immunohistochemical analysis was performed as previously described.<sup>30</sup> Three mAbs against embryonic MyHC were used in this study. mAb 2B6 has been characterized to react specifically with embryonic MyHC.<sup>31</sup> In addition, two mAbs against embryonic MyHC were characterized in this study: mAb 3D1 was raised in our laboratory against cat masseter myosin and was produced according to Lucas et al.<sup>29</sup> and mAb NCL-MHCd (Novocastra Laboratories, Ltd., Newcastle-upon-Tyne, UK) against developmental MyHCs,<sup>32</sup> (abbreviated as NCL-dev in this study). Both mAbs 3D1 and NCL-dev were characterized by Western blot on high-resolution SDS-gels to react with the embryonic MyHC band from the 30-dpc rabbit limb (Figs. 1, 2). One mAb against neonatal MyHC, NCL-MHCn (Novocastra Laboratories, Ltd.),<sup>33</sup> was used (abbreviated as NCL-neo in this study). Two mAbs against EO-specific fast MyHC were used: 4A6<sup>2</sup> and 10A10, which was raised in our laboratory against rabbit EOM MyHC, according to Lucas et al.<sup>29</sup> and has identical specificity on Western blots and muscle sections as 4A6 (data not shown). mAb BA-G5 was raised against cow atrium and reacts with cardiac specific  $\alpha$ -MyHC in rats,<sup>34</sup> obtainable from the American Type Culture Collection (Manassas, VA). In addition we used an mAb against acetylcholinesterase (AChE) to label nerve endings

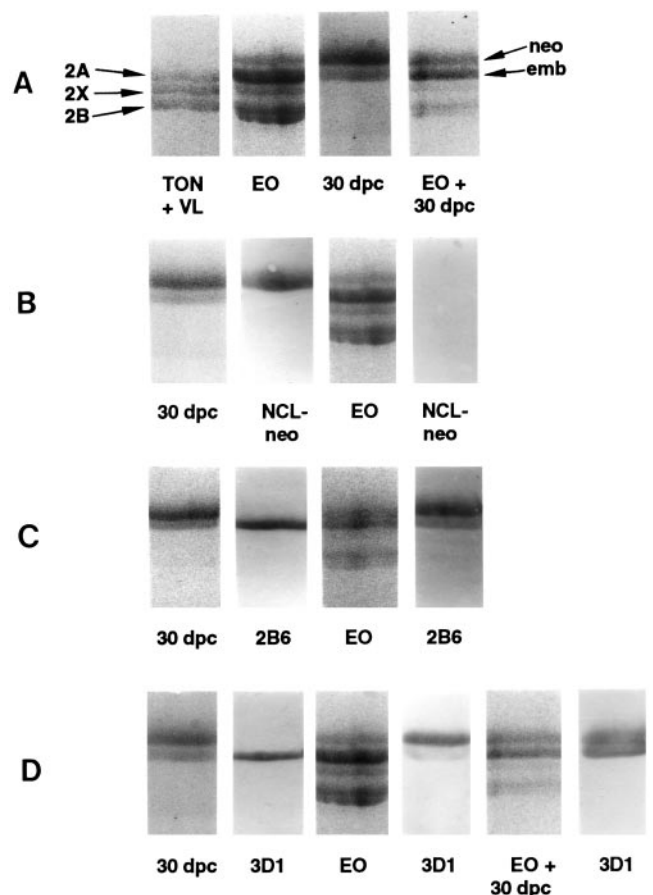


**FIGURE 2.** (A) Protein-stained high-resolution SDS gels of MyHCs from tongue and VL (Ton+VL), extraocular (EO), 30-dpc limb (30 dpc), and EO+30 dpc. (B, C) Protein stained reference gels of 30 dpc and EO and corresponding Western blots stained with mAbs NCL-neo and 2B6 (anti-embryonic MyHC) as labeled. (D) Protein-stained reference gels of 30 dpc, EO, and EO+30 dpc stained with 3D1 (anti-embryonic MyHC) as labeled.

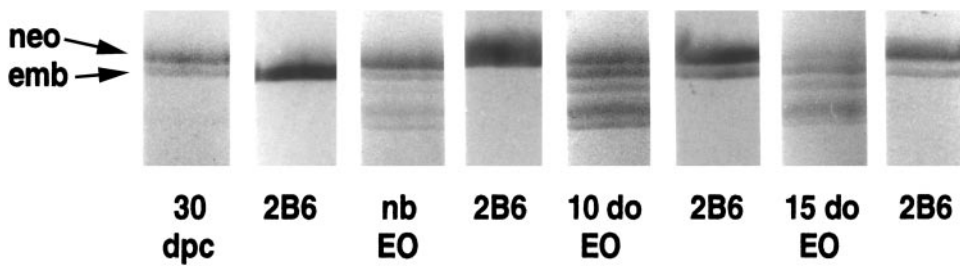


**FIGURE 3.** Protein stained 30-dpc limb, newborn (nb), 10- and 15-day-old (do) EO and corresponding Western blots stained with mAb 2B6 (anti-embryonic MyHC).

(NCL-AchE; Novocastra Laboratories, Ltd.). Horse-radish peroxidase (HRP)-labeled rabbit anti-mouse immunoglobulin antibody (Dako Corp., Carpinteria, CA) was used as a secondary antibody.

### Electrophoretic and Immunoblot Analysis

Myosin used for electrophoretic analysis was extracted as described previously.<sup>35</sup> Myosin was extracted from the distal end of adult EOMs (a mixed population of all rectus and inferior oblique muscles), where developmental MyHCs is known to be expressed in a larger number of muscle fibers.<sup>24</sup> Myosin was also extracted from adult rabbit vastus lateralis, and tongue muscles. Myosin from 30-dpc, newborn, and 10- and 15-day-old whole EOMs (a pooled population of all six EOMs) and limb muscles were also extracted. High-resolution SDS-PAGE was performed according to Talmadge and Roy.<sup>36</sup> Large-format gels were run in a commercial system (Scientific SE 600; Hoeffer Scientific Instruments, San Francisco, CA), with the following slight modifications: 2-mercaptoethanol (10 mM), which is known to improve band resolution,<sup>37,38</sup> was added to the upper electrode buffer, and gels were run for 26 hours, which improved the separation of the embryonic and neonatal MyHCs. The gels were stained with Coomassie brilliant blue. MyHC bands were subjected to Western blot and stained immunohistochemically, as previously described.<sup>39</sup> All Western blot analyses were repeated at least three times.

## RESULTS

### Characterization of mAb NCL-dev

mAb NCL-dev was raised against 7-day-old rat hindlimb muscle myosin and is thought to be against developmental MyHCs (i.e., both embryonic and neonatal MyHCs).<sup>32</sup> This mAb has been shown in immunohistochemical analysis on rabbit EOM sections to have a staining pattern identical with that of an mAb against embryonic MyHC, but distinct from that for anti-neonatal MyHC mAb NCL-neo.<sup>24</sup> We performed high-resolution SDS gel electrophoresis and Western blot analysis to characterize mAb NCL-dev on specific MyHCs from 30-dpc limb muscles of the rabbit. Figure 1 shows SDS-PAGE of MyHCs from rabbit 30-dpc limb muscles stained with Coomassie brilliant blue and corresponding Western blot analysis stained with mAbs NCL-neo and NCL-dev. The 30-dpc limb muscle revealed two MyHC bands. Previous studies applying the Talmadge and Roy<sup>36</sup> gel methodology to the rabbit have shown that neonatal limb MyHC migrates distinctly slower than the embryonic limb MyHC.<sup>40</sup> Thus, the slower-migrating band represents neonatal MyHC and the faster migrating band represents embryonic MyHC. mAb NCL-neo raised against neonatal MyHC<sup>33</sup> stained the slower neonatal MyHC band, whereas mAb NCL-dev stained the faster embryonic MyHC band specifically.

### Identification of Two Electrophoretically Distinct Embryonic MyHC Isoforms in EOM

Figure 2A shows high-resolution SDS-PAGE of MyHCs from rabbit tongue and VL (TON+VL), EO, 30-dpc limb (30 dpc) and

EO+30 dpc muscles stained with Coomassie brilliant blue. Rabbit TON contains predominately 2A MyHC, whereas the VL contains predominately 2X and 2B MyHC.<sup>40</sup> Thus, a mixture of TON+VL separated into three evenly distributed bands corresponding to 2A, 2X, and 2B MyHCs. EO separated into five MyHC bands, the slowest band migrating distinctly slower than the slowest (2A) of the three fast-limb MyHC bands. Myosin from 30 dpc separated into neonatal and embryonic components. The neonatal MyHC band migrated distinctly slower than the 2A MyHC, whereas the embryonic MyHC from 30-dpc limb migrated very close to the 2A MyHC band, consistent with previous studies.<sup>40</sup> The neonatal and embryonic MyHC components in 30-dpc limb comigrated with the two slowest-migrating bands in the EO, as seen in EO+30 dpc.

Figure 2B shows protein stained reference gels of 30 dpc and EO and corresponding Western blots stained with mAb NCL-neo as labeled. mAb NCL-neo stained the slower-migrating band in 30 dpc, but failed to react with EO MyHCs. Thus, although the slower-migrating MyHC band in the EO comigrated with the neonatal MyHC band it was not neonatal MyHC, because it failed to react with the NCL-neo mAb. Figure 2C shows protein-stained reference gels of 30 dpc and EO and corresponding Western blots stained with mAb 2B6 against embryonic MyHC, as labeled. This mAb stained the faster-migrating band in 30 dpc, whereas in EO, it stained the two bands, the MyHC band that comigrated with the embryonic MyHC band in 30 dpc and the slower-migrating band in EO, that comigrated with the neonatal MyHC band in 30 dpc—the latter being more strongly stained than the former. Staining with two other mAbs against the embryonic MyHC, 3D1 (Fig. 2D) and NCL-dev (data not shown), on Western blot analysis of 30 dpc and EO gave similar results. In Western blot analysis of mixtures of EO+30 dpc mAb 3D1 against embryonic MyHC strongly stained the two slowest-migrating bands (Fig. 2D). We thus identified an EO-specific embryonic MyHC in addition to the limb-specific embryonic MyHC in EOM.

### Postnatal Developmental Changes in Expression of Embryonic MyHC Isoforms in the Rabbit EOM

Figure 3 shows protein-stained, high-resolution SDS-PAGE reference gels of 30-dpc limb, newborn, and 10- and 15-day-old EO MyHCs, and corresponding Western blot analysis stained with anti-embryonic MyHC mAb 2B6. mAb 2B6 stained the limb-specific embryonic MyHC (Fig. 3, emb) in 30-dpc limb, but in newborn EO (Fig. 3, nb EO), it stained the slower-migrating EO-specific embryonic MyHC only. In both 10- and 15-day-old EO, mAb 2B6 stained both embryonic MyHC bands, the EO-specific more strongly than the limb-specific, a pattern essentially the same as in the adult (Fig. 2C, 2D).

### Immunohistochemical Analyses of the Expression of Embryonic and Neonatal MyHCs along the Length of the SR

The EOM can be divided into a thin orbital (superficial) region and a larger global (deep) region. The thin orbital layer can be

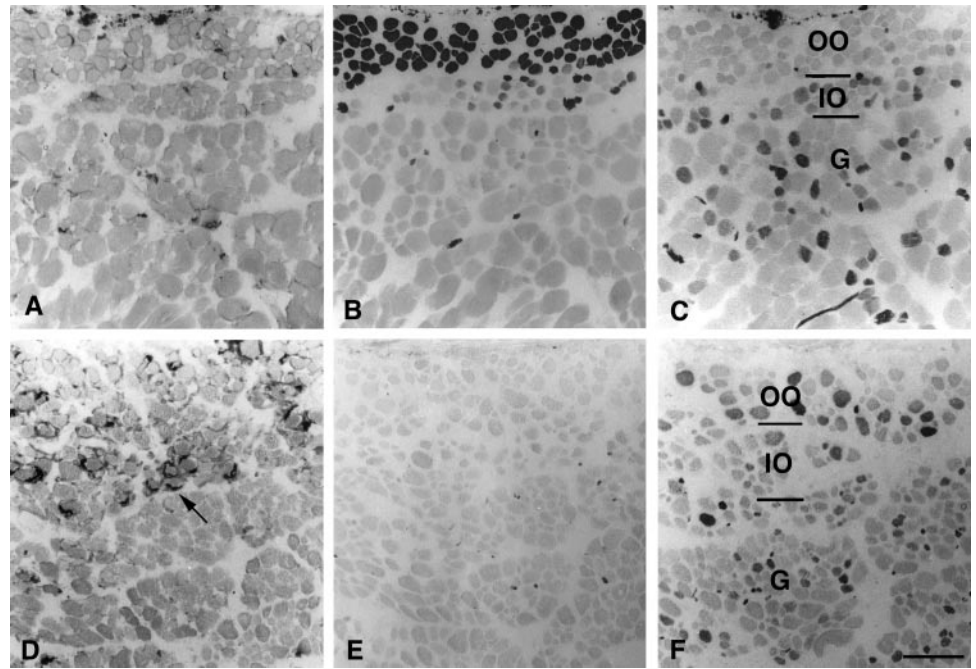


**FIGURE 4.** Immunoperoxidase staining of semiserial sections of the distal region (A–C) and the EPZ (D–F) of the adult rabbit superior rectus, with mAbs NCL-AChE (A, D), NCL-dev (B, E), and NCL-neo (C, F). *Arrow*: an en plaque-like nerve ending (D). OO, outer orbital region; IO, inner orbital region; G, global regions. Scale bar, 100  $\mu$ m.

further subdivided into inner and outer regions (Figs. 4C, 4F). The neuromuscular junctions of rabbit SR orbital muscle fibers were identified by use of an anti-AChE mAb NCL-AChE, and the EPZ was found to be around the middle of the proximal third as described previously.<sup>12</sup> Figure 4 shows the staining patterns of the mAbs NCL-AChE (Figs. 4A, 4D), NCL-dev against the embryonic MyHC (Figs. 4B, 4E), and NCL-neo (Figs. 4C, 4F) distal to the EPZ (Figs. 4A–C) and in the EPZ (Figs. 4D–F). Staining with mAb NCL-AChE in distal sections away from the EPZ showed small superficial en grappe-like nerve endings (Fig. 4A), whereas in the EPZ en plaque-like nerve endings were seen (Fig. 4D). mAb NCL-dev against embryonic MyHC stained almost all muscle fibers in the outer orbital region both distally (Fig. 4B) and proximally (data not shown) away from the EPZ. It also lightly stained a small population of fibers in the inner orbital region. mAb NCL-dev stained very few fibers in the global region distal (Fig. 4B) and proximal (data not shown) to the EPZ, except at the very distal end of the muscle, where an increase in staining was seen in most SR muscles studied (data not shown). Staining with mAb NCL-dev was almost absent in the EPZ in both orbital and global regions (Figs. 4E). mAb NCL-neo stained scattered muscle fibers in the inner orbital and global regions, whereas staining was almost absent in the outer orbital region both distal (Fig. 4C) and proximal (data not shown) to the EPZ. In the EPZ, in contrast to the absence of staining with mAb NCL-dev (Fig. 4E), mAb NCL-neo lightly stained scattered fibers in all three regions (Fig. 4F).

### Immunohistochemical Analyses of the Expression of Other MyHCs in the EPZ of Orbital Fibers

mAb 10A10 against EO-specific fast MyHC stained most of the fibers in the EPZ of the rabbit SR orbital muscle fibers (Fig. 5A). This mAb failed to stain orbital muscle fibers distal (Fig. 5B) and also proximal (data not shown) to the EPZ. mAb 4A6, also against EO-specific fast MyHC, showed the same pattern of staining as mAb 10A10 (data not shown). Figure 5C shows a high-power view of the EPZ stained with anti-EO-specific fast MyHC mAb 10A10. This mAb stained the large-diameter fibers in this region, which are known to be the oSIFs.<sup>12</sup> Complementary to

this, mAb BA-G5 against cardiac  $\alpha$ -MyHC stained the small-diameter fibers (Fig. 5D), which are known to be the oMIFs.<sup>12</sup> Monospecific mAbs against fast (2A, 2B, and 2X) and slow (type 1/ $\beta$ ) MyHCs,<sup>29</sup> as well as a polyclonal antibody specific for slow-tonic MyHC failed to react with SR orbital muscle

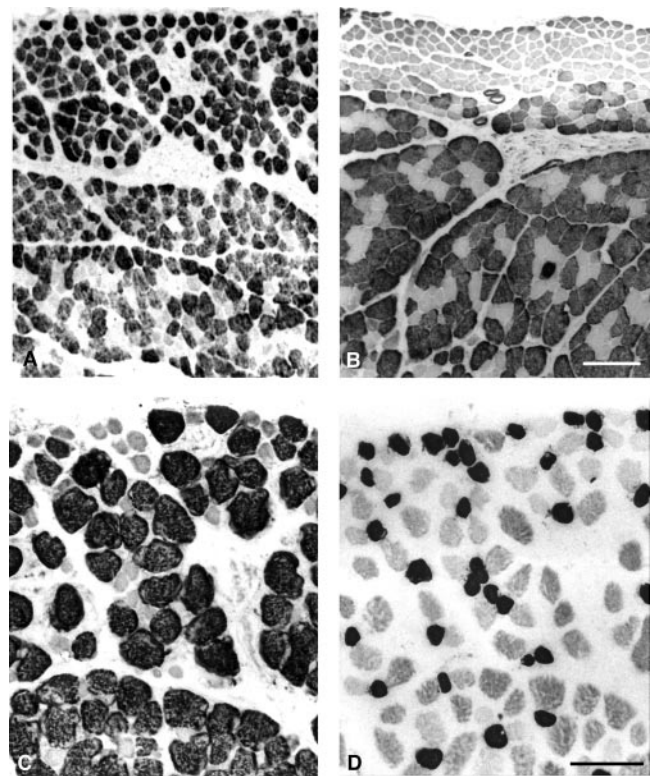


**FIGURE 5.** Immunoperoxidase staining of rabbit superior rectus in the EPZ (A) and the distal region (B) stained with EO-specific fast MyHC mAb 10A10. High-power view of the EPZ (C, D) stained with EO-specific fast MyHC mAb 10A10 (C) and cardiac-specific  $\alpha$ -MyHC mAb BA-G5 (D). Scale bars, 100  $\mu$ m.

fibers in the EPZ (data not shown). Detailed analyses of changes in proportions of fibers expressing different MyHC isoforms along the length of the rabbit SR will be published in subsequent articles.

## DISCUSSION

EOMs are unusual muscles, in that they continue to express embryonic and neonatal/fetal MyHCs in the adult<sup>6</sup> and mAbs NCL-dev and NCL-neo (Novocastra Laboratories, Ltd.) have been valuable probes for studying the expression of developmental MyHCs in EOMs in rat,<sup>21,26</sup> rabbit,<sup>24</sup> and human<sup>41</sup> EOMs. Some of these studies have raised questions as to the specificity of NCL-dev. This mAb was raised against 7-day-old rat hindlimb myosin and reacted with MyHC on low-resolution SDS-PAGE of L6 cells, skeletal muscle from 18-dpc embryonic rats and 7-day-old neonates, but failed to react against adult muscle tissues.<sup>32</sup> It was concluded that this mAb recognizes an epitope present on both the embryonic and neonatal MyHCs.<sup>32</sup> In rabbit<sup>24</sup> and human<sup>41</sup> EOMs, mAb NCL-dev recognizes a distinct population of fiber types from those stained with mAb NCL-neo. Significantly, the pattern of staining for NCL-dev was found to be identical with that for an anti-embryonic MyHC mAb, but whether its specificity was restricted to embryonic MyHC was not investigated.<sup>24</sup> In this study, on high-resolution SDS-PAGE of 30-dpc rabbit limb MyHC, the specificity of mAb NCL-dev was restricted to the embryonic MyHC.

Previous immunohistochemical studies on variation of MyHC expression along the length of rabbit and rat EOM fibers used an mAb that could not distinguish between embryonic and neonatal MyHCs, and the results have suggested that embryonic and/or neonatal MyHC is expressed in the distal and proximal ends of the orbital fibers, but absent in the EPZ.<sup>19,23</sup> In the present study, our analyses showed that this pattern of staining in the rabbit SR reflected the expression of embryonic MyHC and not the neonatal MyHC. Embryonic MyHC was the major developmental MyHC expressed in the outer orbital region of this muscle. It was expressed in most of the outer orbital fibers distal and proximal to the EPZ, but in the EPZ itself, staining was absent. In the global region embryonic MyHC was expressed in very few fibers along the entire length of the SR, except toward the distal and proximal ends where there was an increase in the number of fibers expressing embryonic MyHC, consistent with the results of McLoon et al.<sup>24</sup>

Our analyses also identified the MyHC isoforms that fill in the gap left by the embryonic MyHC in the EPZ of rabbit orbital fibers. EO-fast MyHC was found in the big population of large-diameter fibers in the EPZ. These are identified as oSIFs, which are known to swell in diameter in the EPZ.<sup>12</sup> This pattern of expression of EO-fast MyHC flanked on either side by embryonic MyHC is consistent with previous studies in the rat EOMs,<sup>20</sup> and suggests that such an unusual distribution of MyHC along the length may be characteristic of EO oSIF generally rather than a peculiarity of rat EOM. The small-diameter fibers in the EPZ of the rabbit orbital region are oMIFs, which are known to decrease in diameter at this region.<sup>12</sup> In our analysis, these oMIFs expressed cardiac  $\alpha$ -MyHC in the EPZ.

We found neonatal MyHC expression in rabbit SR too weak to be detected by Western blot analysis. Immunohistochemically, this MyHC was almost absent distal and proximal to the EPZ in the outer orbital layer. A few scattered fibers expressed neonatal MyHC in the EPZ of the outer orbital region, in sharp contrast to the absence of embryonic MyHC in this region. In the global and inner orbital regions, neonatal MyHC was expressed somewhat more abundantly than in the outer orbital layer, where scattered fibers were stained along the entire

length of the SR, consistent with the findings of McLoon et al.<sup>24</sup> The pattern of neonatal MyHC expression in EOMs showed differences across the species. In the rat, neonatal MyHC expression is predominantly found in scattered fibers of the orbital region.<sup>21</sup> In human EOM, however, it is restricted to the outer orbital marginal zone.<sup>41</sup>

Previous electrophoretic analyses of MyHCs in EOMs typically identified MyHC components by matching the electrophoretic mobility of MyHC isoforms in adult and developing limb muscles.<sup>21,25</sup> This approach is hazardous, especially for EOM with its numerous and poorly resolved MyHC components. In this study, the slowest-migrating EOM band comigrated with neonatal MyHC in fetal limb muscle. This EOM band was identified by immunoblot analysis to be an embryonic MyHC isoform and not the neonatal MyHC. Thus this study emphasizes the importance of identifying MyHC components by immunoblot analysis with monospecific antibodies, rather than relying on electrophoretic mobility alone.

Using high-resolution SDS-PAGE and immunoblot analysis of fetal limb and adult EOM MyHCs with three distinct anti-embryonic MyHC mAbs, we characterized two electrophoretically distinct isoforms of embryonic MyHC at the protein level in rabbit EOM: the limb-specific isoform and a second, novel, apparently EOM-specific, isoform. The novel embryonic isoform is the more strongly expressed in adult EOM. As the novel isoform of embryonic MyHC has a lower mobility than the limb-specific isoform, the former is unlikely to be a degradation product of the latter. Neither can it be the slow-tonic MyHC isoform, as a polyclonal antibody against this isoform stained the second fastest-migrating band and not the slowest-migrating band in Western blots of EOM MyHCs. Also, the pattern of staining of the slow-tonic antibody on rabbit EOM sections differs from that of the anti-embryonic MyHC mAbs (Lucas and Hoh, unpublished observations, 2002). The question of heterogeneity of embryonic MyHC in EOM was first raised by the observation of two bands in Western blot analysis of rat EOM using an mAb against embryonic MyHC.<sup>26</sup> However, in this study the two stained bands were not characterized regarding MyHC components in fetal limb and adult EOMs. Although the novel embryonic isoform is found in EOMs, further work on other muscle tissues is necessary to verify the specificity of its expression in EOM.

We found that the expression of the two embryonic isoforms in EOMs undergoes a postnatal developmental change. At birth, only the novel isoform is expressed. By 10 to 15 days the limb-specific isoform is weakly expressed, as found in adult EOMs. We have not ruled out the possibility that the limb-specific embryonic MyHC isoform may be expressed in EOMs at an earlier stage of embryonic development. A pattern of staining of Western blot analysis using an anti-embryonic MyHC antibody in postnatal rat EOMs consistent with the above finding in rabbits has been reported.<sup>26</sup>

The presence of two isoforms of embryonic MyHC in EOM poses questions of their molecular basis and functional significance. The two isoforms could be the products of two embryonic MyHC genes. The mammalian embryonic MyHC gene is a member of a cluster of six fast isoforms arranged in tandem on human chromosome 17 and mouse chromosome 11,<sup>42</sup> and there has not been a report of an additional embryonic MyHC gene. Alternatively, the two embryonic isoforms could be generated by differential splicing of one embryonic MyHC gene. Analysis of limb muscle mRNAs in the fetal pig has revealed two isoforms of embryonic MyHC mRNA. These result from alternate splicing of the full-length message at its 3'-end that results in a 93-amino-acid in-frame deletion, close to the ACD domain, a region that is important for the assembly of myosin filaments.<sup>43</sup> However, in the pig, the truncated isoform of the embryonic MyHC mRNA was found to be the minor isoform in

developing limb muscles, contrary to the expectation based on the predominance of the faster-migrating embryonic MyHC protein isoform in rabbit and rat limb muscle. It remains to be seen whether embryonic MyHC proteins in porcine limb and EOMs are heterogeneous, and whether a similar alternative splicing mechanism could explain EOM embryonic MyHC heterogeneity.

Another possibility for generating two distinct isoforms of embryonic MyHC in EOMs is glycosylation, in which a bulky sugar moiety would be expected to slow mobility in SDS gels. Glycosylation of the masticatory MyHC has been documented,<sup>44</sup> but its functional significance is currently obscure.

Expression of developmental MyHCs in adult limb muscles is generally considered to be an indication of on-going regeneration or arrested development of the muscle. However, expression of embryonic MyHC in adult EOM, specifically in the orbital layer of EOMs, may play an important functional role in eye movements. Measurements on rabbit EOM single fibers have shown a very wide dynamic range of the mechanical parameter  $f_{min}$ , which reflects the kinetics of cross-bridge cycling.<sup>27</sup> The  $f_{min}$ s below and above those in limb fast muscle fibers may be related to the expression of the embryonic and the EO-specific fast MyHCs respectively, which are absent in limb muscles. In this respect, the EO-specific embryonic isoform is likely to play a more important role than the limb-specific isoform, because it occurs in greater abundance. The low level of expression of neonatal MyHC is unlikely to contribute significantly to mechanical properties of EOM fibers.

A common feature of orbital EOM fibers is the occurrence of a kinetically fast segment (the EPZ and central region) flanked by kinetically slower segments on either side. These variations along the length involve not only the contractile machinery, but also structures involved in excitation-contraction coupling. In the rabbit oSIFs, the EPZ contains EO-specific fast MyHC, whereas the flanking segments contain embryonic (present work) and 2A (Lucas and Hoh, unpublished observations, 2002) MyHCs. In the oMIFs, the EPZ contains cardiac-specific  $\alpha$ -MyHC, the central segment contains cardiac-specific  $\alpha$ -MyHC and embryonic MyHCs, and the flanking segments contain embryonic and slow-tonic MyHCs (Lucas and Hoh, unpublished observation, 2002). These arrangements ensure more rapid cross-bridge cycling in the central segments compared with the flanking segments. Further, in oMIFs, the central segment is capable of generating an action potential, whereas the flanking regions are unable to do so.<sup>45</sup> Both the oMIFs<sup>13,16</sup> and oSIFs<sup>14,15,17</sup> display an increase in sarcoplasmic reticulum and express the fast  $Ca^{2+}$ -adenosine triphosphatase (ATPase) pump around the EPZ and central region.<sup>22</sup> These arrangements ensure the rapid release and uptake of  $Ca^{2+}$ , and hence rapid contraction and relaxation, in the EPZ region.

The functional significance of the occurrence of a kinetically fast segment flanked by kinetically slower segments in oMIF and/or oSIFs may be to permit rapid changes in gaze. Consider that these fibers are activated to hold the globe in a given position, and a need arises to change the gaze in the direction that involves relaxation and lengthening of these fibers, as during a saccade in the "off" direction. Without the fast central segment, the slow cross bridges in the relaxing fibers would resist rapid lengthening by developing high tensions as in fibers undergoing eccentric contractions. The resultant high tension would constitute an undesirable load to the antagonist EOM which is trying to shorten at high speed. By having a fast central segment that can relax rapidly, lengthening can be accommodated by the sarcomeres within the EPZ region without an associated rise of tension to oppose the change of gaze.

## Acknowledgments

The authors thank Arthur English (Department of Cell Biology, Emory University School of Medicine, Atlanta, GA) for mAb BA-G5 and Neal Rubinstein (Department of Cell and Developmental Biology, University of Pennsylvania School of Medicine, Philadelphia, PA) for mAb 2B6.

## References

- Porter JD, Baker RS, Ragusa RJ, Brueckner JK. Extraocular muscles: basic and clinical aspects of structure and function. *Surv Ophthalmol*. 1995;39:451-484.
- Lucas CA, Rughani A, Hoh JFY. Expression of extraocular myosin heavy chain in rabbit laryngeal muscle. *J Muscle Res Cell Motil*. 1995;16:368-378.
- Hoh JFY, Hughes S. Myogenic and neurogenic regulation of myosin gene expression in cat jaw-closing muscles regenerating in fast and slow limb muscle beds. *J Muscle Res Cell Motil*. 1988;9:59-72.
- Porter JD, Khanna S, Kaminski HJ, et al. Extraocular muscle is defined by a fundamentally distinct gene expression profile. *Proc Natl Acad Sci USA*. 2001;98:12062-12067.
- Asmussen G, Kiessling A, Wohlrab F. Histochemische Charakterisierung der verschiedenen Muskelfasertypen in den ausseren Augenmuskeln von Säugetieren. *Acta Anat*. 1971;79:526-545.
- Wieczorek DF, Periasamy M, Butler-Browne GS, Whalen RG, Nadal-Ginard B. Co-expression of multiple myosin heavy chain genes, in addition to a tissue-specific one, in extraocular musculature. *J Cell Biol*. 1985;101:618-629.
- Pedrosa-Domellof F, Eriksson PO, Butler-Browne GS, Thornell LE. Expression of alpha-cardiac myosin heavy chain in mammalian skeletal muscle. *Experientia*. 1992;48:491-494.
- Rushbrook JI, Weiss C, Ko K, et al. Identification of alpha-cardiac myosin heavy chain mRNA and protein in extraocular muscle of the adult rabbit. *J Muscle Res Cell Motil*. 1994;15:505-515.
- Sartore S, Mascarello F, Rowlerson A, et al. Fibre types in extraocular muscles: a new myosin isoform in the fast fibres. *J Muscle Res Cell Motil*. 1987;8:161-172.
- Pierobon-Bormioli S, Torresan P, Sartore S, Moschini GB, Schiaffino S. Immunohistochemical identification of slow tonic fibres in human extrinsic eye muscles. *Invest Ophthalmol Visual Sci*. 1979;18:303-306.
- Pierobon-Bormioli S, Sartore S, Vitadello M, Schiaffino S. Slow myosins in vertebrate skeletal muscle: an immunofluorescence study. *J Cell Biol*. 1980;85:675-681.
- Davidowitz J, Phillips G, Breinin GM. Organization of the orbital surface layer in rabbit superior rectus. *Invest Ophthalmol Visual Sci*. 1977;16:711-729.
- Davidowitz J, Chiarandini DJ, Phillips G, Breinin GM. Morphological variation along multiply innervated fibers of rat extraocular muscles. In: Lennnerstrand G, Zee DS, Keller EL, eds. *Functional Basis of Ocular Motility Disorders*. Oxford, UK: Pergamon Press; 1982:17-26.
- Pachter BR. Fiber composition of the superior rectus extraocular muscle of the rhesus macaque. *J Morphol*. 1982;174:237-250.
- Pachter BR. Rat extraocular muscle. 1. Three dimensional cytoarchitecture, component fibre populations and innervation. *J Anat*. 1983;137:143-159.
- Davidowitz J, Phillips G, Breinin GM. Variation of mitochondrial volume fraction along multiply innervated fibers in rabbit extraocular muscle. *Tissue Cell*. 1980;12:449-457.
- Pachter BR, Davidowitz J, Breinin GM. Light and electron microscopic serial analysis of mouse extraocular muscle: morphology, innervation and topographical organization of component fiber populations. *Tissue Cell*. 1976;8:547-560.
- Davidowitz J, Rubinson K, Jacoby J, Phillips G. Myofibril size variation along the length of extraocular muscle in rabbit and rat I. orbital layer. *Tissue Cell*. 1996;28:63-76.
- Jacoby J, Ko K, Weiss C, Rushbrook JI. Systematic variation in myosin expression along extraocular muscle fibres of the adult rat. *J Muscle Res Cell Motility*. 1990;11:25-40.
- Rubinstein NA, Hoh JFY. The distribution of myosin heavy chain isoforms among rat extraocular muscle fiber types. *Invest Ophthalmol Vis Sci*. 2000;41:3391-3398.

21. Kranjc BS, Sketelj J, D'Albis A., Ambroz M., Erzen I. Fibre types and myosin heavy chain expression in the ocular medial rectus muscle of the adult rat. *J Muscle Res Cell Motil.* 2000;21:753-761.
22. Jacoby J, Ko K. Sarcoplasmic reticulum fast Ca<sup>2+</sup>-Pump and myosin heavy chain expression in extraocular muscles. *Invest Ophthalmol Vis Sci.* 1993;34:2848-2858.
23. Jacoby J, Ko K, Davidowitz J, Weiss C, Rushbrook JI. Systematic expression of alpha-cardiac myosin in multiply-innervated fibres of extraocular muscle. *Soc Neurosci Abstr.* 1990;16:119.
24. McLoon LK, Rios L, Wirtschafter JD. Complex three-dimensional patterns of myosin isoform expression: differences between and within specific extraocular muscles. *J Muscle Res Cell Motil.* 1999;20:771-783.
25. Asmussen G, Traub I, Pette D. Electrophoretic analysis of myosin heavy chain isoform patterns in extraocular muscles of the rat. *FEBS Lett.* 1993;335:243-245.
26. Brueckner JK, Itkis O, Porter JD. Spatial and temporal patterns of myosin heavy chain expression in developing rat extraocular muscle. *J Muscle Res Cell Motil.* 1996;17:297-312.
27. Li Z B, Rossmann GH, Hoh JFY. Cross-bridge kinetics of rabbit single extraocular and limb muscle fibres. *Invest Ophthalmol Vis Sci.* 2000;41:3770-3774.
28. Schiaffino S, Reggiani C. Molecular diversity of myofibrillar proteins: gene regulation and functional significance. *Physiol Rev.* 1996;76:371-423.
29. Lucas CA, Kang LH, Hoh JFY. Monospecific antibodies against the three mammalian fast limb myosin heavy chains. *Biochem Biophys Res Commun.* 2000;272:303-308.
30. Hoh JFY, Hughes S, Hale PT, Fitzsimons RB. Immunocytochemical and electrophoretic analyses of changes in myosin gene expression in cat limb fast and slow muscles during postnatal development. *J Muscle Res Cell Motil.* 1988;9:30-47.
31. Gambke B, Rubinstein NA. A monoclonal antibody to the embryonic myosin heavy chain of rat skeletal muscle. *J Biol Chem.* 1984;259:12092-12100.
32. Davis CE, Harris JB, Nicholson LVB. Myosin isoform transitions and physiological properties of regenerated and re-innervated soleus muscles of the rat. *Neuromuscul Disord.* 1991;1:411-421.
33. Ecob-Prince M., Hill M., Brown W. Immunocytochemical demonstration of myosin heavy chain expression in human muscle. *J Neurol Sci.* 1989;91:71-78.
34. Rudnicki MA, Jackowski G, Saggin L, McBurney MW. Actin and myosin expression during development of cardiac muscle from cultured embryonal carcinoma cells. *Dev Biol.* 1990;138:348-358.
35. Hoh JFY, Yeoh GPS. Rabbit skeletal myosin isoenzymes from foetal, fast-twitch and slow-twitch muscles. *Nature.* 1979;280:321-323.
36. Talmadge RJ, Roy RR. Electrophoretic separation of rat skeletal muscle myosin heavy-chain isoforms. *J Appl Physiol.* 1993;75:2337-2340.
37. Fritz JD, Swartz DR, Greaser ML. Factors affecting polyacrylamide gel electrophoresis and electroblot analysis of high-molecular-weight myofibrillar proteins. *Anal Biochem.* 1989;180:205-210.
38. Blough ER, Rennie ER, Zhang F, Reiser PJ. Enhanced electrophoretic separation and resolution of myosin heavy chains in mammalian and avian skeletal muscles. *Anal Biochem.* 1996;233:31-35.
39. Lucas CA, Hoh JFY. Extraocular fast myosin heavy chain expression in the levator palpebrae and retractor bulbi muscles. *Invest Ophthalmol Vis Sci.* 1997;38:2817-2825.
40. Janmot C, d'Albis A. Electrophoretic separation of developmental and adult rabbit skeletal muscle myosin heavy chain isoforms: example of application to muscle denervation study. *FEBS Lett.* 1994;353:13-15.
41. Wasicky R, Ziya-Ghazvini F, Blumer R, Lukas JR, Mayr R. Muscle fibre types of human extraocular muscles: a histochemical and immunohistochemical study. *Invest Ophthalmol Vis Sci.* 2000;41:980-990.
42. Weiss A, McDonough D, Wertman B, et al. Organization of human and mouse skeletal myosin heavy chain gene clusters is highly conserved. *Proc Natl Acad Sci.* 1999;290:61-75.
43. Sun YM, DaCosta N, Birrell R, Archibald AL, Alzuherri H, Chang KC. Molecular and quantitative characterisation of the porcine embryonic myosin heavy chain gene. *J Muscle Res Cell Motil.* 2001;22:317-327.
44. Kirkeby S. A monoclonal anticarbohydrate antibody detecting superfast myosin in the masseter muscle. *Cell Tissue Res.* 1996;283:85-92.
45. Jacoby J, Chiarandini DJ, Stefani E. Electrical properties and innervation of fibers in the orbital layer of rat extraocular muscles. *J Neurophysiol.* 1989;61:116-125.